AAPS PharmSciTech, Vol. 15, No. 4, August 2014 (© 2014)
DOI: 10.1208/s12249-014-0112-0

Research Article

Enhancing the Antitumor Activity of Berberine Hydrochloride by Solid Lipid Nanoparticle Encapsulation

Lu Wang,[1] Hongtao Li,[2] Shengpeng Wang,[1] Rong Liu,[2] Zhisheng Wu,[3] Chunming Wang,[1,4] Yitao Wang,[1] and Meiwan Chen[1,4]

Received 11 November 2013; accepted 13 March 2014; published online 3 April 2014

Abstract. Berberine hydrochloride (BH) is an isoquinolin alkaloid with promising anticancer efficacies. Nevertheless, further development and application of this compound had been hampered by its poor aqueous solubility, low gastrointestinal absorption, and rapid metabolism in the body. In this study, a solid lipid nanoparticle (SLN)-based system was developed for efficient incorporation and persistent release of BH. The drug-loading SLNs (BH-loaded SLNs) were stable, with a mean particle size of 81.42±8.48 nm and zeta potential of −28.67±0.71 mV. BH-loaded SLNs showed desirable drug entrapment efficiency and drug-loaded, and the release of BH from SLNs was significantly slower than free BH. Importantly, our *in vitro* study indicated that BH-loaded SLNs more significantly inhibited cell proliferation on MCF-7, HepG 2, and A549 cancer cells. Meanwhile, clone formation, cellular uptake, cell cycle arrest, and cell apoptosis studies also demonstrated that BH-loaded SLNs enhanced the antitumor efficacies of BH on MCF-7 cancer cells. Taken together, our results suggest that this SLN formulation may serve as a novel, simple, and efficient system for the delivery of BH.

KEY WORDS: antitumor evaluation; apoptosis; berberine hydrochloride; solid lipid nanoparticles.

INTRODUCTION

Berberine hydrochloride (BH) (Fig. 1a) is an isoquinolin alkaloid found in numerous common medicinal plants such as the Berberidaceae and Ranunculaceae families (1,2). It has various pharmacological effects including antiinflammatory (3), antimicrobial (4), and antipyretic activities (5). Until now, BH has been widely used for treating diabetic renopathy (6), mycotic infection (7), heart and cardiovascular diseases (8,9), and lung disease in clinic (10). Besides, pilot studies in evaluation of the antitumor effect of BH demonstrated that this compound could inhibit proliferation of cancer cells, induce cell cycle at G1/G0 phase, and induce apoptosis in cancer cells (11,12). However, further development and application of this compound has encountered several challenges, particularly *in vivo*, largely due to its poor aqueous solubility, low gastro-intestinal absorption, and rapid metabolism (13,14). A potential solution to these obstacles is to utilize nanoparticulate formulations, which have been demonstrated to enhance bioavailability and efficacies of loaded water-insoluble drugs (15). Among them, solid lipid nanoparticles (SLNs) qualify as a suitable candidate carrier. SLNs have been increasingly used since the early 1990s. They can be made from biodegradable solid lipids in submicron size by high-pressure homogenization method (16–18). As potential drug carriers, SLNs are suitable for improving bioavailability and/or achieve sustained delivery of drugs. Such formulations possess high biocompatibility and low toxicity and are easy to fabricate and cheap (19,20). Many other studies have showed that, as delivery vehicles, SLNs could improve drug targeting and protect incorporated compound against degradation as well as preclude remain of organic solvent (21–24). Therefore, in the present study, we aimed to design, optimize, and establish an SLN-based system for efficient incorporation and controlled release of BH. We particularly investigated the drug-release kinetics of this system and further evaluated its antitumor effects on various cancer cells *in vitro*.

MATERIALS AND METHODS

Materials

BH (98%) purity was provided by Nanjing spring and autumn Biological Technology Co. Ltd. (Nanjing, China). Glyceryl monostearate was obtained from Tianjin Bodi Chemical Limited Co. (Tianjin, China). Tween 80 was purchased from Chemical Reagent Factory of Guangzhou (Guangzhou, China) and Dulbecco's Modified Eagle Medium (DMEM) was obtained from Gibico Life Technologies (MD, USA). Penicillin-streptomycin (PS), fetal

Lu Wang and Hongtao Li contributed equally to this work.

[1] State Key Laboratory of Quality Research in Chinese Medicine, Institute of Chinese Medical Sciences, University of Macau, Av. Padre Tomas Pereira S.J., Taipa, 999078Macau, China.
[2] State Key Laboratory of Respiratory Diseases, First Affiliated Hospital of Guangzhou Medical College, 510120, Guangzhou, China.
[3] Beijing University of Chinese Medicine, 100102, Beijing, China.
[4] To whom correspondence should be addressed. (e-mail: CMWang@umac.mo; chenmeiwan81@163.com)

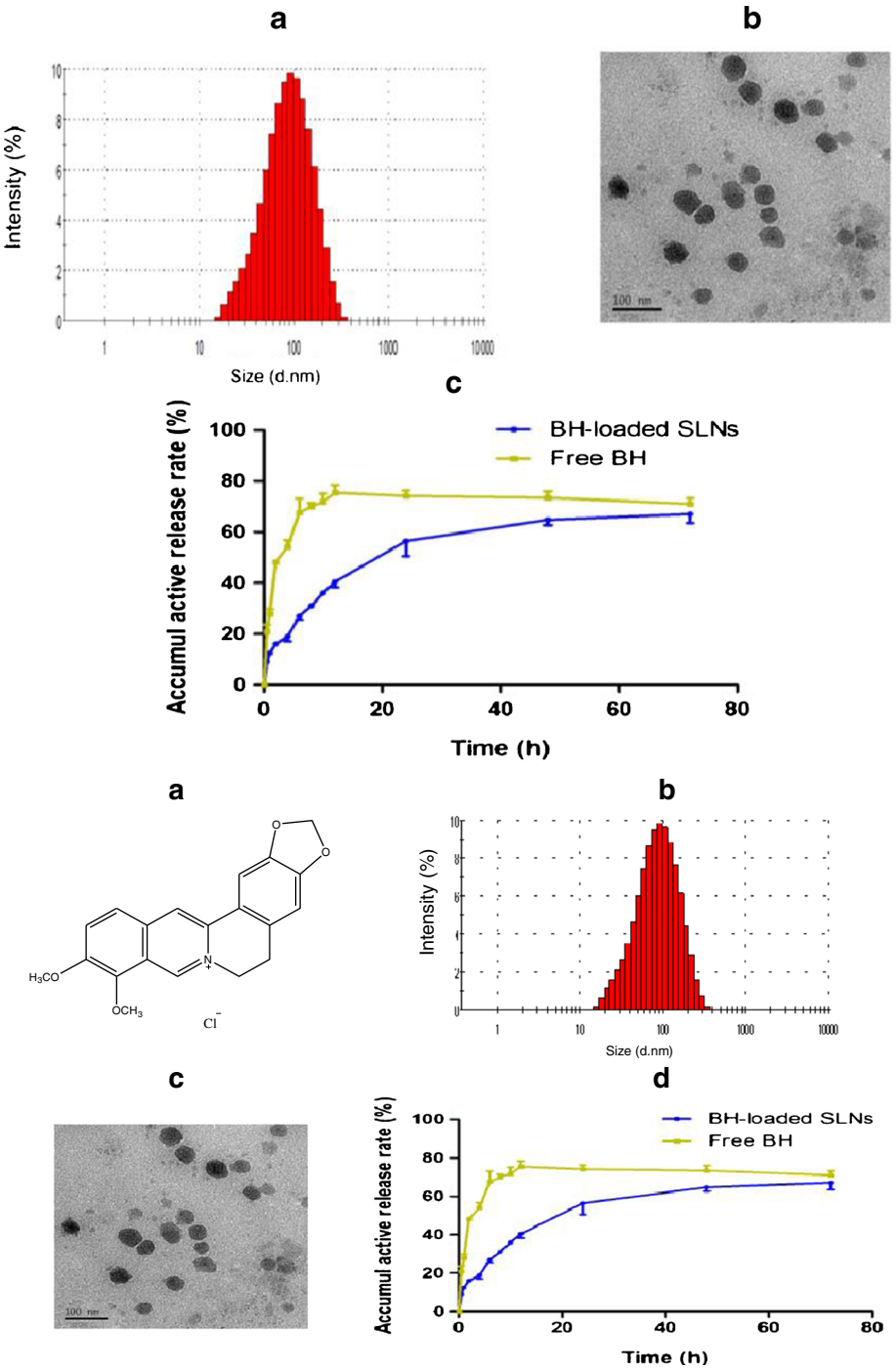

Fig. 1. The chemical structure of BH (**a**), particle size (**b**), and TEM morphology (**c**) of BH-loaded SLNs. Drug release profiles of BH-loaded SLNs and free BH for 72-h duration time (**d**)

bovine serum (FBS), phosphate-buffered saline (PBS), 0.25% (*w*/*v*) trypsin/1 mM ethylene diamine tetraacetic acid (EDTA), propidium iodide (PI), and Hoechst 33342 were supplied from Invitrogen (Carlsbad, CA, USA). 3-(4, 5-Dimethylthiazol-2-yl)-2, 5-diphenyltetrazolium bromide (MTT) was obtained from Molecular Probes (Eugene, USA). Annexin V-FITC/PI apoptosis detection kit was purchased from Biovision Incorporated Company. Coumarin 6 and paraformaldehyde (PFA) were obtained by Sigma-Aldrich (St. Louis, MO, USA). Other chemicals were of analytical grade from local sources and used with no further purification.

Preparation of BH-Loaded SLNs

The BH-loaded SLNs were prepared by a high-pressure homogenization method (25). 1,000 mg glyceryl monostearate (melting point at 81°C) was heated 5–10°C above its melting point, and then 400 mg Tween 80 was added in to the lipid phase, which was previously heated at the same temperature.

During the homogenization process, the temperature was maintained around 80°C to guarantee that the lipid material does not solidify. Following, a pre-emulsion was obtained by stirring at 8,000 rpm for 30 min. This pre-emulsion was further passed through by a high-pressure homogenizer (APV2000, Denmark) at 1,000 bar for 12 cycles. Then, the obtained SLNs were transferred to glass vials and cooled down immediately to room temperature to maintain the stability of SLNs. For BH-loaded SLNs, the drug around 33 mg was added to the solid lipid before melting and homogenization. All the samples were stored in refrigerator at 4°C.

Characterization of BH-Loaded SLNs

HPLC Analysis of BH

The content of BH in various mediums was analyzed using high-performance liquid chromatography (HPLC) method. 4.60 mm×250 mm, i.d., 5 μm particle size, Agilent Eclipse XDB-C18 column was used for the detection of BH content. A mobile phase containing a mixture of acetonitrile and 0.05 mol/l NaH_2PO_4 (pH 2.5 adjusted by phosphoric acid) (30:70 *v*/*v*) was pumped through Waters e2695 HPLC system equipped with a photodiode array detector Waters 2998 at a flow rate of 1.0 ml/min. The UV detection was performed at 345 nm with a temperature of 30°C. The volume of injection was 10 μl and the retention time of BH was about 7 min. The temperature of the column was maintained at 30°C. HPLC tests demonstrated that a sensitive quantitative assay of BH with a calibration linear curve indicated over a concentration range of 4.0–256.0 μg/ml (r^2=1).

Particle Size and Zeta Potential

The average particle size and size distribution of BH-loaded SLNs were determined by A Zetasizer-Nano-ZSP (Malvern, UK) at room temperature. After being diluted 10 times with double-distilled water, samples were measured to obtain the data of its particle sizes, while there is no dilution underwent before the measurement of its zeta potential. Furthermore, all the results presented were conducted at least three times for accuracy. Besides, the sample was prepared by placing a drop of diluted 50-fold BH-loaded SLNs with double-distilled water onto a 400-mesh copper grid coated with carbon film and then followed by negative staining with 1% phosphotungstic acid. After air drying, the shape and size of BH-loaded SLNs was obtained by transmission electron microscopy (TEM).

Determination of Drug Encapsulation Efficiency and Loading Content

Encapsulation efficiency (EE) of BH-loaded SLNs was calculated by determining the amount of free BH using centrifugal ultrafiltration technique. Firstly, 2-ml BH-loaded SLN colloidal solution was placed into a centrifuge tube matched and centrifuged for 45 min at 4,500 rpm. The liquid supernatant was filtered by 0.45-μm microporous filtering membrane and then kept as unencapsulated BH sample for further detection. Secondly, the total BH content in BH-loaded SLNs was determined as follows: aliquots of 2-ml BH-loaded SLN dispersion were dissolved and diluted appropriately by methanol to dissolve the SLNs. After the same centrifugal method, the obtained suspension was allowed to filter through 0.45-μm membrane filters and kept as total BH in BH-loaded SLNs. Thirdly, the ultrafiltrates containing the unencapsulated BH and total BH contents of BH-loaded SLNs were determined by HPLC detector (method was detailed in HPLC analysis of BH) separately. Finally, the drug loading content (DLC) and EE was calculated by these equations as follow:

$$EE = \frac{W_B - W_U}{W_B} \times 100\ \%$$

$$DLC = \frac{W_B - W_U}{W_B - W_U + W_S} \times 100\%$$

In detail, W_B represents for the amount of BH used for each sample, W_U represents for the amount of unencapsulated BH after centrifugation, and W_S was the weight of lipid added during the whole system.

In Vitro Drug Release Studies

BH release from SLNs was performed using the dialysis bag method. Phosphate buffer (PBS, pH 7.4) with 0.2% (*w*/*v*) sodium dodecyl sulfate (SDS) was served as dissolution medium. The dialysis bag (Biotopped, USA) could retain nanoparticles and allow the diffusion of free drug into dissolution media. The bags were soaked in double-distilled water for 8 h before use. Of BH-loaded SLN dispersion, 2 ml was poured into the bag with the two ends fixed by clamps. Then, the bags were placed in a 50-ml centrifuge tube, and 25 ml fresh dissolution media was added into it. The centrifuge tubes were placed into a thermostatic shaking incubator (Labnet, American) at 37°C at a rate of 120 rpm. At 0.5, 1, 2, 4, 6, 8, 10, 12, 24, 48, and 72 h of the time points, 0.5 ml of the mediums in the conical flask were removed for analysis and same amount of fresh dialysis medium was then added to maintain the conditions. The drug contents in samples were analyzed by detailed HPLC method. All the operations were carried out in triplicate, and the cumulative percentages of the release profiles of free BH and BH-loaded SLNs were calculated.

Antitumor Efficacy of BH-Loaded SLNs

Cell Culture

The human breast cancer cell line (MCF-7), human hepatocellular carcinoma cell line (HepG 2), human lung carcinoma cell line (A549), and human mammary epithelial cell line (MCF-10A) were purchased from American Type Culture Collection (ATCC). All cells were cultured in DMEM medium with antibiotics (100 U/ml penicillin and 100 μl/ml streptomycin) and 10% (*v*/*v*) heat-inactivated FBS at 37°C containing 5% CO_2.

Assessment of Cell Viability by MTT Assay

MTT colorimetric assay is capable of detecting viable cells by the decrease of the yellow tetrazolium salt to purple formazon (26). MCF-7 cells (0.6×10^4), HepG 2 cells (0.8×10^4),

A549 cells (0.8×10^4), and MCF-10A cells (0.8×10^4) were seeded in 96-well plate, respectively, and incubated for 24 h to be allowed to attach to plates. After 24 h of incubation, cells were treated with free BH, BH-loaded SLNs, blank SLNs, and free BH spiked with blank SLNs at different concentrations for 24 and 48 h, respectively to detect the value of IC_{50}. After respective incubation periods, the cell viabilities were detected by the medium containing MTT (1 mg/ml) for 4 h at 37°C. Then, the generated formazan crystals were dissolved by dimethylsulfoxide (100 μl/well) and determined by a microplate reader at 570 nm (Molecular Devices, USA). The optical density value of processed cells presented the percentage of cell survival in corresponding wells, contrasting with respective controls.

Plate Clone Forming Experiment

MCF-7 cells (2.0×10^5) were seeded in a 5-ml flask for 24 h of incubation and then added with free BH, BH-loaded SLNs, blank SLNs, and free serum group for 48 h of incubation. Subsequently, cells of each group were de-aggregated and then the single cell suspensions of each group were resuspended into 6-well plate with the cell concentration of 6×10^2/well. After cultured at 37°C with 5% CO_2 for 20 days, the cells in each well were slowly washed by PBS twice and then fixed with 4% PFA for 10 min. Then visible clone clusters were dyed with crystal violet and then resuspended in PBS for taking pictures.

Study of Cellular Uptake

The cellular uptake efficiency of BH-loaded SLNs formulations was detected by flow cytometry (BD, USA). The insoluble fluorescent dye, coumarin 6, was loaded into SLNs with the same BH-loading method. After being seeded into 6-well plate for 24 h of incubation at 37°C in a humidified atmosphere containing 5% CO_2, MCF-7 cells (1.2×10^6) were added with serum-free medium that contains free coumarin 6 and coumarin 6-loaded SLNs (the coumarin 6 concentration was 100 ng/ml). With 1, 2, and 4 h of incubation, cells were collected and washed twice with PBS and then the fluorescence of coumarin 6 in cells were evaluated by flow cytomery with FITC channel. On the other hand, MCF-7 (0.8×10^4) were seeded into 96-well plate and incubated for 24 h. Then, the same dosages of coumarin 6 and coumarin 6-loaded SLNs with free serum medium were added into each well. Subsequently, followed by 1, 2, and 4 h of incubations, cells were washed twice with PBS and then fixed with 4% PFA for 12 min. The nucleus of cells were dyed by Hoechst 33342 for 10 min and then washed with PBS twice. After being resuspended in PBS solution, cells were detected by Incell 2000 Analyzer.

Determination of Cell Cycle Arrest by Flow Cytometer

The analysis of cell cycle distribution can determine the contents of DNA to identify whether cell cycle arrest has happened (27). MCF-7 cells (1.2×10^6) were seeded in 6-well plates and incubated for 24 h. After 24 h of starvation, cells were treated with free BH, BH-loaded SLNs, and blank SLNs at different concentrations for another 48 h, respectively. After incubation, cells were washed twice with PBS, harvested, and collected by centrifugation at 500*g* for 5 min, then fixed in 70% ice-cold ethanol under −20°C overnight. After that, cells were collected by centrifugation and resuspended in 100 μL PI stain solution (20 μg/ml PI, 8 μg/mlDNase-free RNase) each well for 20 min without light. By analyzing with a flow cytometer (BD FACS CantoTM, BD Biosciences, San Jose, USA), the cell distributions of the phases of G0/G1, S, and G2/M were detected and the results were analyzed by the version 3.0 ModFited LT software.

Hoechst 33342 Staining

MCF-7 cells (0.6×10^4) were seeded into 96-well plates and incubated for 24 h. After cells had attached to plates, BH, BH-loaded SLNs, and blank SLNs in different concentrations were added into corresponding wells. Cells were incubated for another 48 h and then fixed with 4% paraformaldehyde for 10 min at 4°C. Then, cells were washed by PBS twice and stained with 1 μg/ml Hoechest 33342 at room temperature for 20 min. Cells were washed and re-suspended in PBS for morphologic observation by using Incell 2000 analyzer (GE Healthcare, USA).

Determination of Cell Apoptosis by Annexin V/PI Staining Assay

MCF-7 cells were treated with different concentrations of BH, BH-loaded SLNs, and blank SLNs solutions for 48 h, respectively. Then cells were collected after being treated with trypsin solution and centrifugation, and then washed twice with cold PBS and re-suspended in 100 μl binding buffer. After 15 min incubation in the dark at room temperature, collected cells were added with 3 μl Annexin V-FITC and 5 μl PI and then analyzed by a flow cytometer (BD FACS CantoTM, BD Biosciences, San Jose, USA). Then, cell apoptosis could be detected, which could show the early apoptotic stage with the graph symbol Annexin V^+ and PI^-, and the late apopotic stage with the graph symbol of Annexin V^+ and PI^+.

Statistical Analysis

All experiments were carried out in triplicate, and all data obtained were expressed as mean±standard error. Statistical comparisons were performed by analysis of variance using student *t* test method. Values of $p\leq0.01$ or $p\leq0.05$ were considered statistically significant.

RESULTS AND DISCUSSION

Determination of Particle Size and Zeta Potential

The particle size, polydispersity index (PDI), zeta potential of BH-loaded SLNs, and blank SLNs formulation were measured by a zetasizer (ZSP, Malvern, UK). BH-loaded SLNs were prepared by using glyceryl monostearate and Tween 80, and the data presented indicated that BH-loaded SLNs possessed a stable condition with a narrow PDI value (Table I). In detail, the mean particle size of BH-loaded SLNs was 81.42±8.48 nm, which is a little higher than blank SLNs (68.43±10.84 nm) (Fig. 1b). The slight increase in particle size

Table I. Characteristics of the Formulation of BH/Blank SLNs

Nanoparticles	Particle size (nm±SD)	PDI (±SD)	Zeta potential (mV±SD)	EE (%±SD)	DLC (%±SD)
BH-loaded SLNs	81.42±8.48	0.25±0.03	−28.67±0.71	70.33±1.53	2.85±0.04
Blank SLNs	68.43±10.84	0.26±0.04	−29.80±0.36	–	–

Results are given as mean±SD (n=3)
SD standard deviation, *PDI* polydispersity index, *EE* encapsulation efficiency, *DLC* drug loading content, *BH* berberine hydrochloride, *SLNs* solid lipid nanoparticles

of BH-loaded SLNs might results from the entrapment of free BH into SLNs. On the other hand, the zeta potential of BH-loaded SLNs was −28.67±0.71 mV, which was similar with blank SLNs (−29.80±0.36 mV). Zeta potential of BH-loaded SLNs indicated that it exhibited a very good stability for loading free BH. Besides, the morphology of BH-loaded SLNs showed that it presented a spherical or nearly orbicular shapes and homogeneous size, which visually detailed the specific physical characteristics of BH-loaded SLNs (Fig. 1c). All the data presented demonstrated that BH-loaded SLNs could be a stable drug carrier with narrow particle size, steady zeta potential, and closely graded shape.

Drug Encapsulation Efficiency and Loading Content

The EE and DLC of BH were detected by the HPLC method mentioned above. In this study, we found that the EE% of the formulation of BH-loaded SLNs was 70.33±1.53% and the DLC reached to 2.85±0.04% (Table I). Considered the long centrifugation time of BH-loaded SLNs, the actual EE% might be higher than the values of detection for BH leak-out could occur under high eccentricity condition. Nevertheless, Table I verified that the BH-loaded SLNs formulation hold an excellent loading quality in our study and it may help BH keep effective forms and function well during

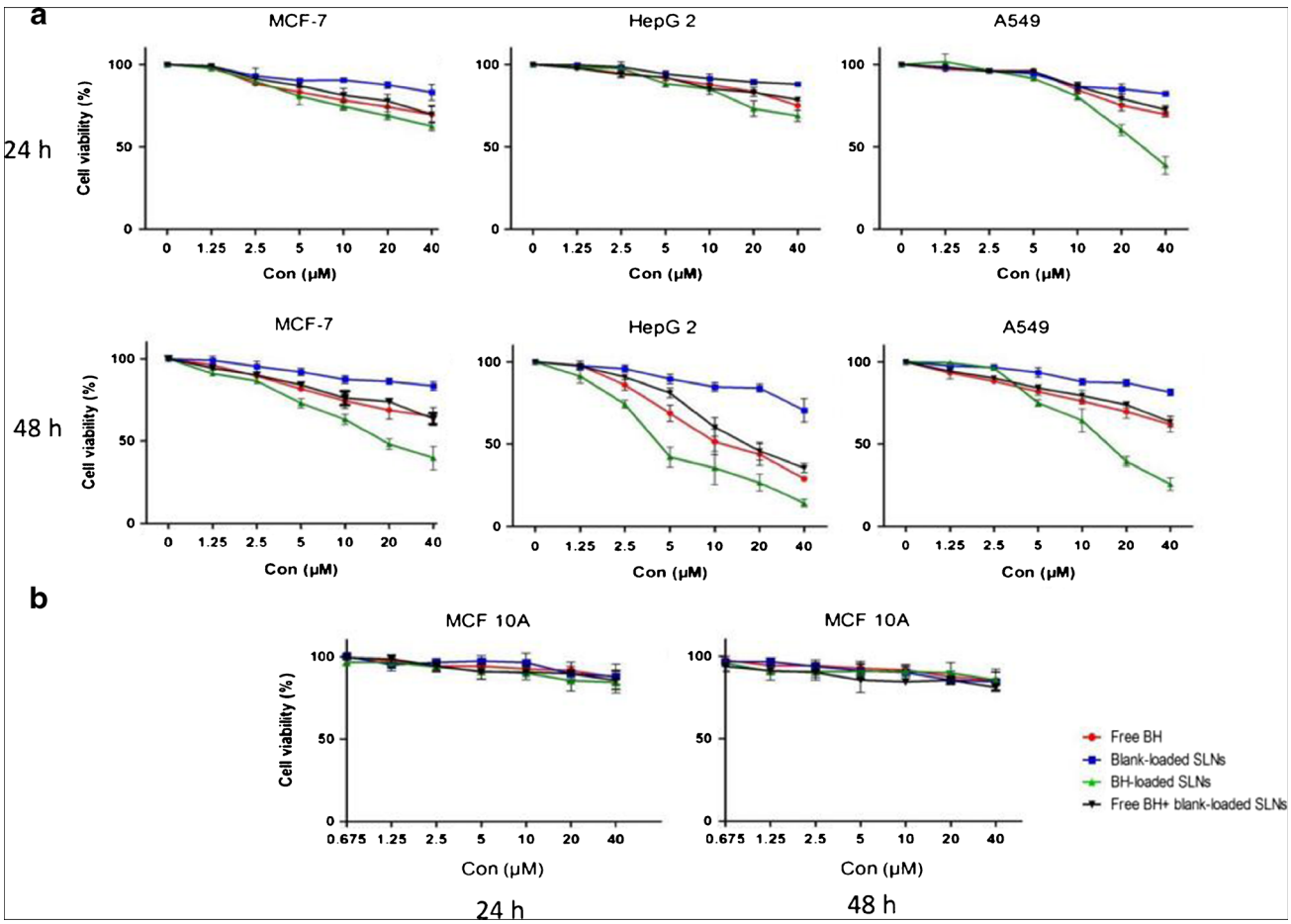

Fig. 2. **a**, **b** MTT assay showed different viabilities of MCF-7, HepG 2, A549, and MCF 10A treated with free BH and BH-loaded SLNs (0–40 μM) at different time points (24, 48 h). Blank SLNs treatment (0–40 μM), free BH (0–40 μM), and free BH spiked with blank SLNs were presented for comparison reference. Data were obtained by at least three times repeated trials

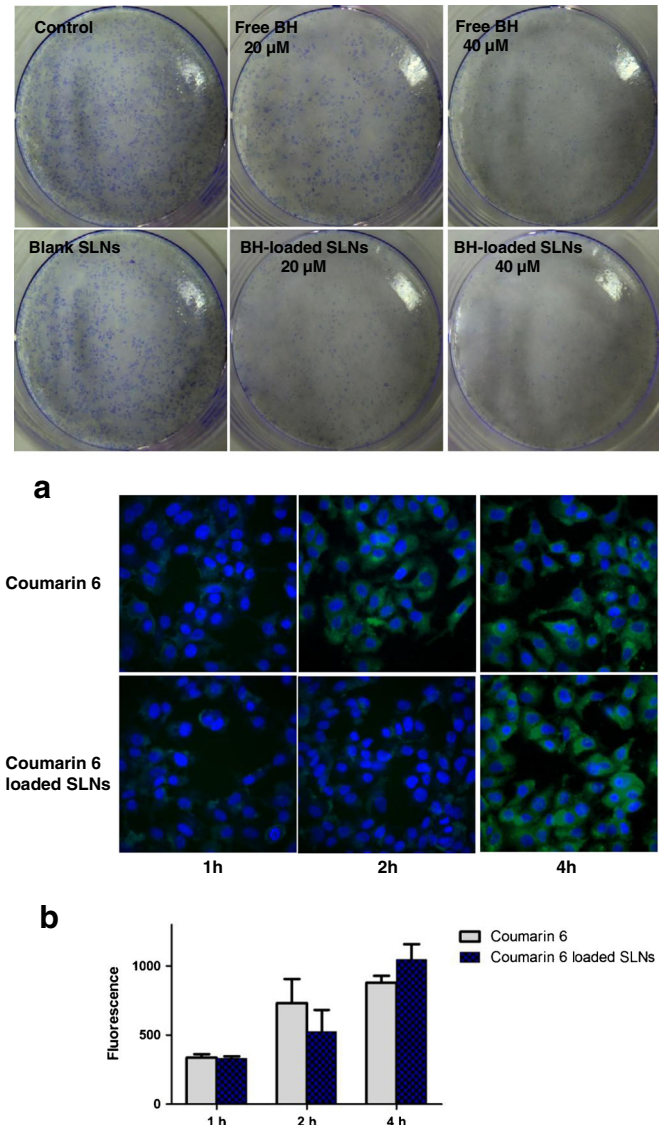

Fig. 3. Clone formation results incubated for 20 days. Cells were treated with 20 and 40 μM coumarin 6 and coumarin6-loaded SLNs, compared with serum-free and blank SLNs

the absorption, distribution, metabolism, and excretion period for further clinical use.

In Vitro Drug Release Properties

The BH-loaded SLNs release profile *in vitro* was carried out in PBS (pH 7.4) with 2% sodium dodecyl sulfate for 72 h duration of time. The release profile presented in Fig. 1d showed an initial burst release during 0.5 to 6 h on free BH groups, while there exhibited a slow release on BH-loaded SLNs groups. Furthermore, the data of drug release rate indicated that the slow release of BH-loaded SLNs had lasted for nearly 48 h. Besides, the cumulative release rates showed that the steady release percentages of free BH had reached above 75% while there that of BH-Loaded SLNs was almost 60%. It was deduced that there was some BH adhered to the surface and in SLNs. This phenomenon could illustrate that the BH-loaded SLNs indeed could provide a slow release performance for BH and it has a great potential applicability as BH carrier to keep providing during the treatment.

Antitumor Efficacy of BH-Loaded SLNs

BH-Loaded SLNs Enhanced the Antiproliferation Effect

In our study, the human breast cancer cell line (MCF-7), human hepatocellular carcinoma cell line (HepG 2), human lung carcinoma cell line (A549), and human mammary epithelial cell line (MCF-10A) were treated with different dosages of free BH, BH-loaded SLNs, and blank SLNs for 24 and 48 h. Figure 2a presented that both free BH and BH-loaded SLNs could significantly suppress the proliferation of MCF-7 cells, HepG 2 cells, and A549 cells in dose- and time-dependent manner. For 24 h of treatment, BH-loaded SLNs presented a

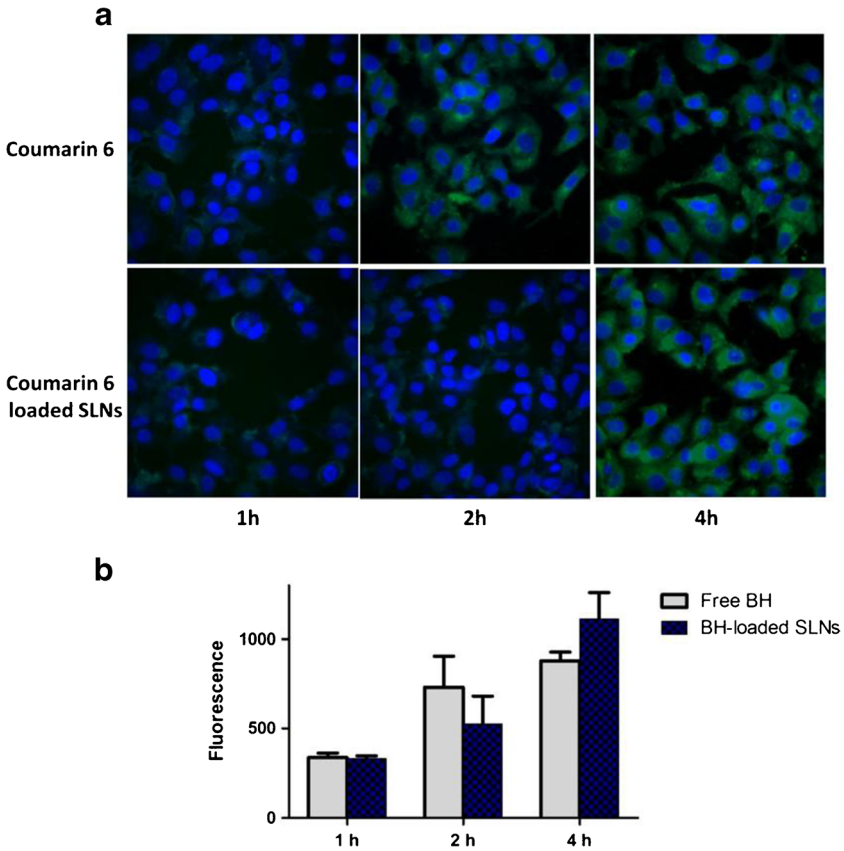

Fig. 4. Cellular uptake images of MCF-7 cells treated with 20 and 40 μM free BH and BH-loaded SLNs (**a**) and fluorescence values of MCF-7 detected by flow cytometry (**b**) for 1-, 2-, and 4-h treatment time

significantly higher inhibition rates (61.8%) on MCF-7 cells compared with free BH at 40 μM (76.8%), blank SLNs (88.9%), and free BH spiked with blank SLNs (76.2%) groups. On HepG 2 cells, BH-loaded SLNs presented a significantly higher inhibition rates (68.9%) of cells at 40 μM compared with free BH (75.9%), blank SLNs (93.1%), and free BH spiked with blank SLNs (79.9%) groups. There were a significant inhibition of BH-loaded SLNs on A549 cells (42.1%) at 40 μM compared with the corresponding free BH group (72.5%), blank SLNs group (83.5%), and the physical mixed group (75.3%). For 48 h of treatment, the IC_{50} of BH-loaded SLNs on MCF-7, HepG 2, and A549 were 20.5, 4.8, and 15.2 μM, respectively, on free BH were above 40, 10.3, and 40 μM, respectively, and on free BH mixed with blank SLNs were above 40, 16.7, and above 40 μM, respectively. After 48 h of treatment, the cell viabilities of BH-loaded SLNs were all showed much lower than free BH at each dosage. Furthermore, Statistics showed that the longer incubation time cells were taken, the more significant variance of proliferous inhibition BH-loaded SLNs would be displayed compared with free BH group and free BH spiked with blank SLNs groups. The different cell viabilities of BH-loaded SLNs and the physical mixed SLNs indicated that BH encapsulated in SLNs had significant inhibition of proliferation on MCF-7, HepG 2, and A549 cells, which might be due to it had a higher uptake ability of cancer cells and its sustained release effect of SLNs (28). Specifically, incubation of MCF-7 cells with 40 μM BH-loaded SLNs for 24 and 48 h had showed significant less cell viability of MCF-7 compared with free BH, which is chosen as the high dosage for the next experiments for SLN formulation IC_{50} is above 40 μM and has significant inhibition on proliferation of MCF-7. Besides, all values are compared with normal breast cells MCF 10A studies and showed low toxicity during all cell viability experiments (Fig. 2b).

To further confirm the inhibition results of BH-loaded SLNs, clone formation experiments were taken and results indicated that the 40 μM BH-loaded SLNs could significantly inhibit the clone formation of MCF-7 cells compared with all the other groups presented (Fig. 3).

Study of Cellular Uptake by MCF-7 Cells

Cellular uptake of BH-loaded SLNs and free BH in MCF-7 cells were presented by images and quantified by flow cytometry (Fig. 4). The uptake degree of free BH-treated cells rapidly raised at about 2 h while it was obviously increased after 4 h of BH-loaded SLNs treatment. The gradual uptake of BH-loaded SLNs in 4 h reflected that there existed a sustained release of SLNs. For free BH, it was presented that the speed of the uptake degrees of 2 to 4 h of treatment time were increased slower than the period from the beginning to 1 h of incubation, and these phenomenon might results from the exocytosis of MCF-7 cells. For BH-loaded SLNs, the uptake degree at 4 h was significantly augmented compared with the

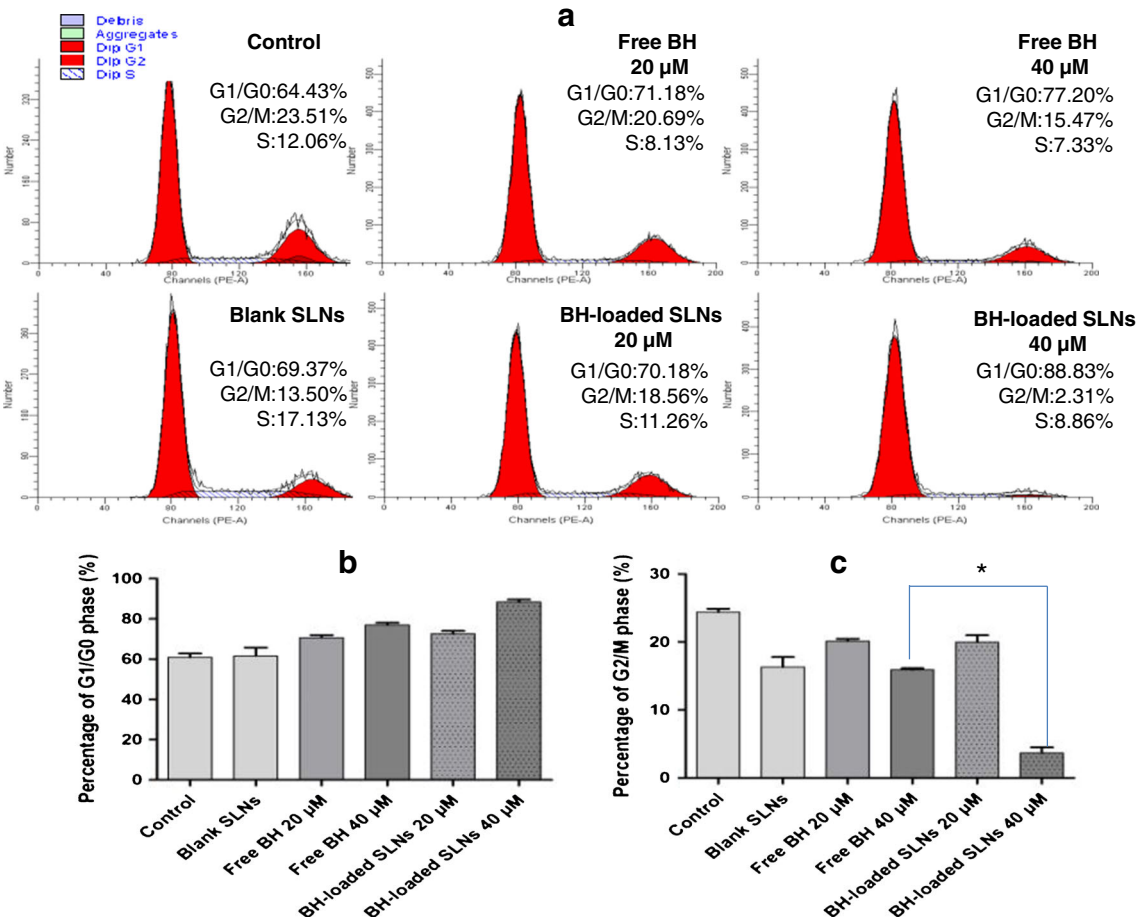

Fig. 5. **a**–**c** Cell cycle distributions of MCF-7 cells treated with different solutions (free BH and BH-loaded SLNs) at different concentrations (40 and 20 μM) compared with control and blank SLNs for 48 h. Free BH and BH-loaded SLNs arrested MCF-7 cells at G1/G0 phase and induced significant decrease at S and G2/M phase. Data were expressed as mean±standard error. *$p<0.05$ *vs.* control

previous testing times and this phenomenon was speculated results from the sustained release of coumarin 6 and the increased endocytosis and less exocytosis of MCF-7 cells.

BH-Loaded SLNs Induced Cell Cycle Arrest in MCF-7 Cells

The mechanism of cell inhibition induced by BH has been tested on different kinds of cancer cells (29–33). In order to investigate whether the decreased growth rate of the treated MCF-7 cell was due to cell cycle arrest, we analyzed the data of PI-stained cells by using flow cytometry with MCF-7. As shown in Fig. 5, treated with BH and BH-loaded SLNs at 40 and 20 μM, MCF-7 cancer cells had showed significant accumulation of cells at G1/G0 phase as compared to the control and blank SLNs. More specifically, for the G1/G0 phase, 40 μM BH-loaded SLNs treated cell fractions increased to 88.83% compared with blank SLNs (69.37%) and control cells (64.43%), indicating that BH and BH-loaded SLNs arrested the cells at G1/G0 phase and thereby prevented cell cycle progression to G2/M phase. The G2/M phase of MCF-7 cells was significantly decreased after 48 h of treatment of 40 μM BH-loaded SLNs (2.31%) compared with blank SLNs (13.50%) and control cells (12.06%). In addition, the percentages of G1/G0 cell cycle arrest of BH-loaded SLNs on 20 μM had no obvious difference with 20 μM free BH, suggesting that BH-loaded SLNs only had stronger delay or inhibition of cell cycle progression at G1/G0 phase on high-concentration treatment. In summary, it was convinced that BH-loaded SLNs had more significant function of arresting cell cycle than free BH at high tested dosage (40 μM).

BH-Loaded SLNs Treatment Induced Apoptosis in MCF-7 Cells

Hoechst 33342, as a DNA minor groove binding ligand, could display apoptosis of different cancer cells through detecting its variations of fluorescence degree and the shapes of fluorescence (34). To further verify that BH-loaded SLNs induce apoptosis of MCF-7, Hoechst 33342 was used to stain MCF-7 cells processed by different solutions of free BH and BH-loaded SLNs at 20 and 40 μM concentrations for efficient comparative analysis with Annexin V-FITC and PI-staining method. Cells in BH-loaded SLNs and free BH groups showed an increased bright fluorescence while cells in control and blank SLNs groups displayed a weak fluorescence and had slight morphologic changes. MCF-7 cancer cells in 40 μM BH-loaded SLNs showed low livability, abundant typical apoptotic bodies, and cells crenulation (Fig. 6). In summary,

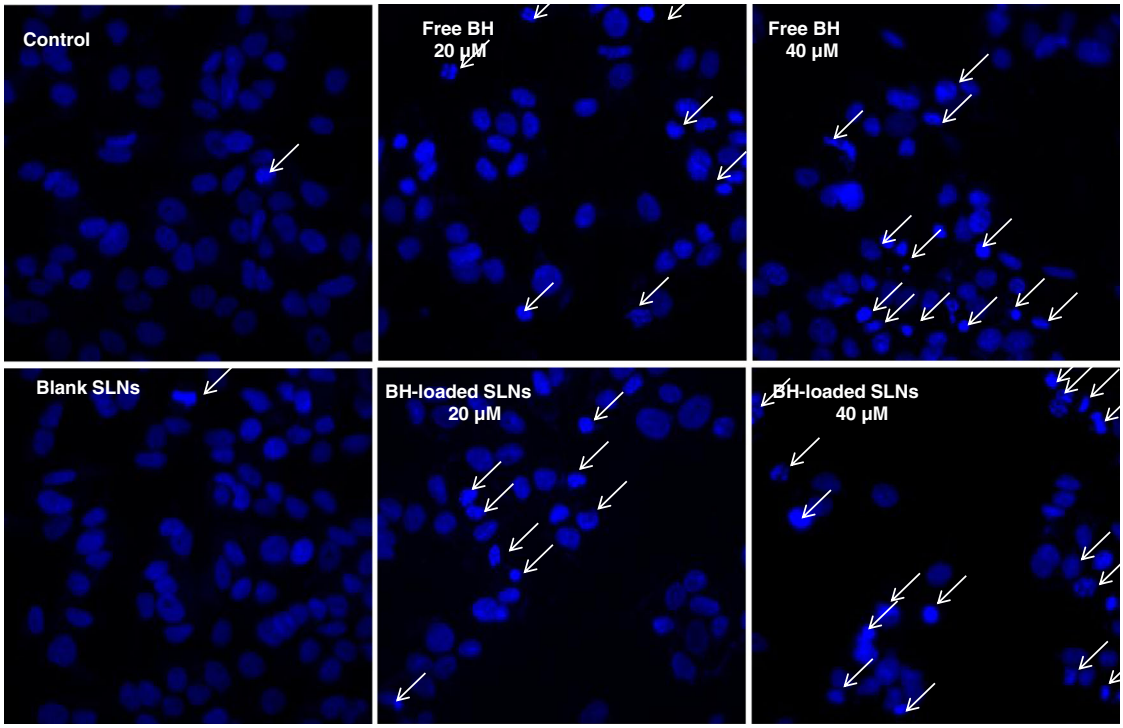

Fig. 6. Apoptotic morphology in MCF-7 cells treated with free BH and BH-loaded SLNs for 48 h were detected by Hoechst 33342 fluorescent staining with fluorescence microscopy

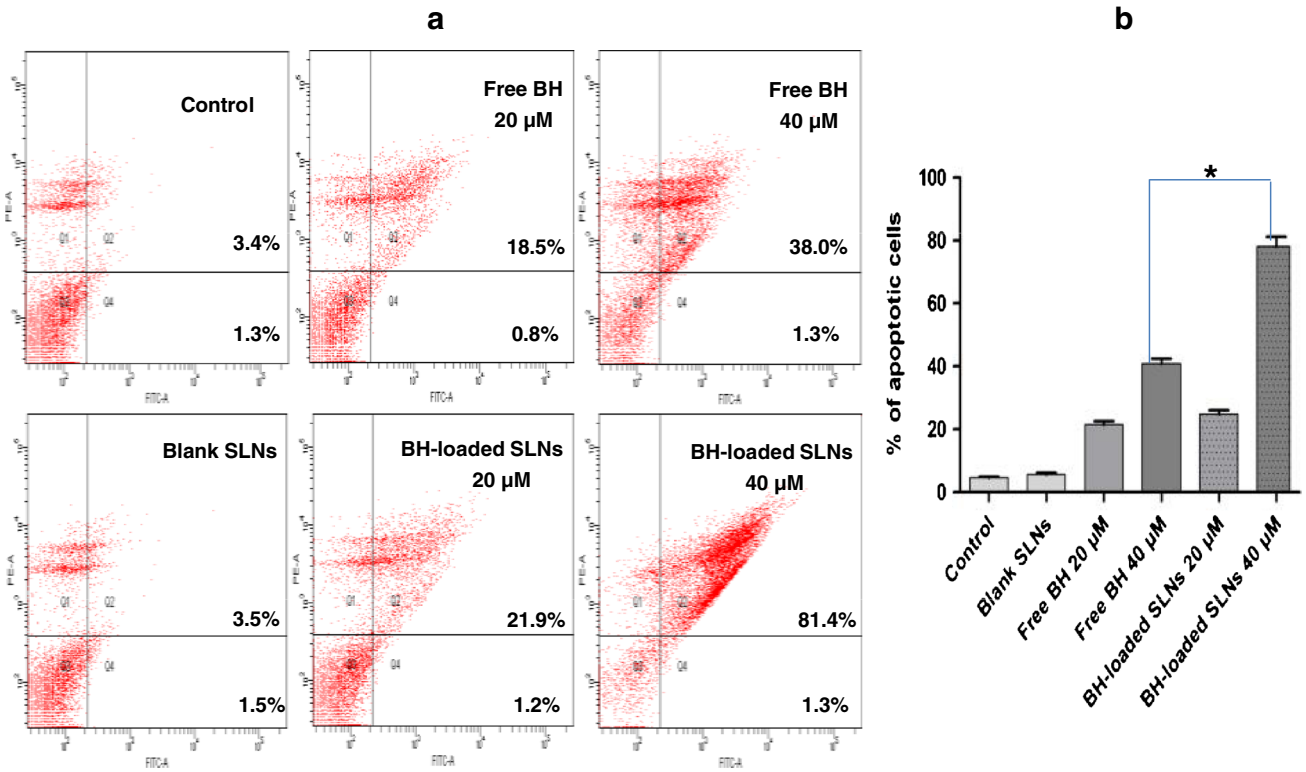

Fig. 7. Cell apoptosis of MCF-7 cells after treatment of free BH and BH-loaded SLNs at 20- and 40-μM concentrations for 48 h (**a**) and the histogram of apoptotic degrees (Q2 and Q4 phase) of MCF-7 treated with 20 and 40 μM free BH and BH-loaded SLNs for 48 h (**b**). Necrotic cells (Q1 Annexin V-FITC-PI+), late apoptotic (Q2 Annexin V-FITC-PI+), live cells (Q3 Annexin V-FITC-PI-), and early apoptotic cells (Q4 Annexin V-FITC+PI-)

obvious fluorescence in BH-loaded SLNs indicated that the apoptotic effects were enhanced by SLNs preparations.

Flow cytometry with Annexin V-FITC and PI staining could effectively distinguish early apoptosis from late apoptosis or necrosis. Early apoptotic cells could be detected by fluorescently labeled Annexin V, for Annexin V has a high affinity towards phosphatidyl serine. Meanwhile, because of the permeability through the damaged cell membranes, PI could be used to detect necrotic cells (35). Based on the results of Hoechst 33342 staining, we further characterized and quantified the BH/BH-loaded SLNs-induced apoptosis by Annexin V/PI dual staining. Percentages of cells in each quadrant are representative of necrotic cells (Q1 Annexin V-FITC-PI+), late apoptotic (Q2 Annexin V-FITC-PI+), live cells (Q3 Annexin V-FITC-PI-), and early apoptotic cells (Q4 Annexin V-FITC+PI-) (Fig. 7a). The percentages of early apoptotic cells (Annexin V-FITC positive cells) were obviously increased after the treatment of BH and BH-loaded SLNs. Fig. 7a showed that the early and late apoptotic cell populations (Q2 and Q4 phase) after 40 μM BH-loaded SLNs treatment significantly increased up to 81.4 and 1.3%, respectively, compared with 40-μM free BH treatment showed as 38.0 and 1.3%, and 20-μM BH-loaded SLNs treatment increased up to 21.9 and 1.2%, respectively, compared with 20-μM free BH treatment showed as 18.5 and 0.8%, while those treated by blank SLNs and control group all were below 5.0%. These findings demonstrated that 40 μM BH-loaded SLNs could markedly induce early and late apoptosis in MCF-7 cells (Fig. 7b). Furthermore, compared with free BH-treated group at each concentration, BH-loaded SLNs had a more obvious apoptotic phenomenon at early apoptosis.

CONCLUSIONS

To summarize, the developed BH-loaded SLNs demonstrated good stability with small nanoparticle size and stable zeta potential, controlled drug release rate compared with free BH, and low toxicity of blank SLNs by MTT assay. In contrast to free BH, BH-loaded SLNs showed stronger effect on reducing the growth rate and more significant induction of cell cycle arrest and apoptosis on MCF-7 breast cancer cells. Increased uptake rate of coumarin-6-loaded SLNs compared with free coumarin 6 demonstrated that SLNs was an effective deliver to carry BH into MCF-7 cells, which could be an important reason that contributes to enhancement of antitumor activity of BH. Our work provided evidence for the possibility of BH-loaded SLNs as a stable, safe, and practical drug delivery system for potential cancer treatment. Next, investigating how to prolong drug residence time to 48 h in the body in vivo models will be planned and conducted in our following researches. We recommend further study be focused on specific experiments on the oral formulation of BH *in vivo* in order to improve the actual pharmacological activities and extend applications of BH.

ACKNOWLEDGMENTS

This study was supported by the Macao Science and Technology Development Fund (102/2012/A3) and the Research Fund of the University of Macau (SRG025-ICMS13-CMW).

REFERENCES

1. Li AR, Zhu Y, Li XN, Tian XJ. Antimicrobial activity of four species of Berberidaceae. Fitoterapia. 2007;78(5):379–81.
2. Guo ZG, Lin Z, Sun RQ, Sun SQ, Wang LQ. Analysis of contents of berberine in Coptis chinensis of Lichuan. Zhongguo Yi Xue Ke Xue Yuan Xue Bao. 2004;26(6):618–21.
3. Zhou H, Mineshita S. The effect of berberine chloride on experimental colitis in rats in vivo and in vitro. J Pharmacol Exp Ther. 2000;294(3):822–9.
4. Iwasa K, Lee DU, Kang SI, Wiegrebe W. Antimicrobial activity of 8-alkyl- and 8-phenyl-substituted berberines and their 12-bromo derivatives. J Nat Prod. 1998;61(9):1150–3.
5. Kupeli E, Kosar M, Yesilada E, Husnu K, Baser C. A comparative study on the anti-inflammatory, antinociceptive and antipyretic effects of isoquinoline alkaloids from the roots of Turkish berberis species. Life Sci. 2002;72(6):645–57.
6. McCarthy N, Mitchell G, Bilous M, Wilcken N, Lindeman GJ. Triple-negative breast cancer: making the most of a misnomer. Asia Pac J Clin Oncol. 2012;8(2):145–55.
7. Albal MV, Jadhav S, Chandorkar AG. Clinical evaluation of berberine in mycotic infections. Indian J Ophthalmol. 1986;34 (1):91–2.
8. Zeng X. Relationship between the clinical effects of berberine on severe congestive heart failure and its concentration in plasma studied by HPLC. Biomed Chromatogr. 1999;13(7):442–4.
9. Derosa G, Maffioli P, Cicero AF. Berberine on metabolic and cardiovascular risk factors: an analysis from preclinical evidences to clinical trials. Expert Opin Biol Ther. 2012;12(8):1113–24.
10. Lin K, Liu S, Shen Y, Li Q. Berberine attenuates cigarette smoke-induced acute lung inflammation. Inflammation. 2013;2013 (1):1–8.
11. Fukuda K, Hibiya Y, Mutoh M, Koshiji M, Akao S, Fujiwara H. Inhibition by berberine of cyclooxygenese-2 transcriptional activity in human colon cancer cells. Ethnopharmacology. 1999;66(2):227–33.
12. Jow SJ, Cha LC. Study on the physical and chemical properties of berberine as related to the biological effects. I. Acid dissociation constant. Yao Xue Xue Bao. 1965;12(9):571–6.
13. Rawat DS, Thakur BK, Semalty M, Semalty A, Badoni P, Rawat MS. Baicalein-phospholipid complex: a novel drug delivery technology for phytotherapeutics. Curr Drug Discov Technol. 2013;10 (3):1–9.
14. Oh YJ, Choi G, Choy YB, Park JW, Park JH, Lee HJ, *et al.* Aripiprazolemontmorillonite: a New organic–inorganic nanohybrid material for biomedical applications. Chemistry. 2013;19(15):4869–75.
15. Parveen R, Ahmad FJ, Iqbal Z, Samim M, Ahmad S. Solid lipid nanoparticles of anticancer drug andrographolide: formulation, in vitro and in vivo studies. Drug Dev Ind Pharm. 2013;2(1):2–9.
16. Gokce EH, Korkmaz E, Dellera E, Sandri G, Bonferoni MC, Ozer O. Resveratrol-loaded solid lipid nanoparticles versus nanostructured lipid carriers: evaluation of antioxidant potential for dermal applications. Int J Nanomedicine. 2012;7(1):1841–50.
17. Liu DY, Luo DF, Ye JT. Study on preparation of ginsenoside-Rd solid lipid nanoparticles. Chin J Hosp Pharm. 2010;30(1):25–30.
18. Ju H, Hao CJ, Yin F, Song LL, Chen CL, Xiao L. Preparation and characterization of curcumin solid lipid nanoparticles. Drug Eval Res. 2010;33(6):420–3.
19. Chen C, Fan T, Jin Y, Zhou Z, Yang Y, Zhu X, *et al.* Orally delivered salmon calcitonin-loaded solid lipid nanoparticles prepared by micelle-double emulsion method via the combined use of different solid lipids. Nanomedicine (London). 2012;8(7):1–16.
20. Cai S, Yang Q, Bagby TR, Forrest ML. Lymphatic drug delivery using engineered liposomes and solid lipid nanoparticles. Adv Drug Deliv Rev. 2011;63(10–11):901–8.
21. Priano L, Zara GP, El-Assawy N, Cattaldo S, Muntoni E, Milano E, *et al.* Baclofen-loaded solid lipid nanoparticles: preparation, electrophysiological assessment of efficacy, pharmacokinetic and tissue distribution in rats after intraperitoneal administration. Eur J Pharm Biopharm. 2011;79(1):135–41.
22. Silva AC, Gonzalez-Mira E, Garcia ML, Egea MA, Fonseca J, Silva R, *et al.* Preparation, characterization and biocompatibility studies on risperidone-loaded solid lipid nanoparticles (Sln): high

pressure homogenization versus ultrasound. Colloids Surf B: Biointerfaces. 2011;86(1):158–65.
23. Loredana S, Roberto C, Macrco D, Raffaello S, Germana M, Elisabeta M, *et al*. Solid lipid nanoparticles as anti-inflammatory drug delivery system in a human inflammatory bowel disease whole-blood mode. Eur J Pharm Sci. 2010;39(5):428–36.
24. Kumar VV, Chandrasekar D, Ramakrishna S, Kishan V, Rao YM, Diwan PV. Development and evaluation of nitrendipine loaded solid lipid nanoparticles: influence of wax and glyceride lipids on plasma pharmacokinetics. Int J Pharm. 2007;335(1–2):167–75.
25. Wang S, Chen T, Chen R, Hu Y, Chen M, Wang Y. Emodin loaded solid lipid nanoparticles: preparation, characterization and antitumor activity studies. Int J Pharm. 2012;430(1–2):238–46.
26. Ahmadian S, Barar J, Saei AA, Fakhree MA, Omidi Y. Cellular toxicity of nanogenomedicine in Mcf-7 cell line: Mtt assay. J Vis Exp. 2009;1(26):1–2.
27. Jin X, Tang S, Chen Q, Zou J, Zhang T, Liu F, *et al*. Furazolidone induced oxidative DNA damage via up-regulating Ros that caused cell cycle arrest in human hepatoma G2 cells. Toxicol Lett. 2011;201(3):205–12.
28. Jenning V, Thunemann AF, Gohla SH. Characterisation of a novel solid lipid nanoparticle carrier system based on binary mixtures of liquid and solid lipids. Int J Pharm. 2000;199(2):167–77.
29. Chai YS, Hu J, Lei F, Wang YG, Yuan ZY, Lu X, *et al*. Effect of berberine on cell cycle arrest and cell survival during cerebral ischemia and reperfusion and correlations with P53/cyclin D1 and Pi3k/Akt. Eur J Pharmacol. 2013;02(41):44–55.
30. Wang Y, Liu Q, Liu Z, Li B, Sun Z, Zhou H, *et al*. Berberine, a genotoxic alkaloid, induces Atm-Chk1 mediated G2 arrest in prostate cancer cells. Mutat Res. 2012;734(1–2):20–9.
31. He W, Wang B, Zhuang Y, Shao D, Sun K, Chen J. Berberine inhibits growth and induces G1 arrest and apoptosis in human cholangiocarcinoma Qbc939 cells. J Pharmacol Sci. 2012;119(4):341–8.
32. Yan K, Zhang C, Feng J, Hou L, Yan L, Zhou Z, *et al*. Induction of G1 cell cycle arrest and apoptosis by berberine in bladder cancer cells. Eur J Pharmacol. 2011;661(1–3):1–7.
33. Lin JP, Yang JS, Lee JH, Hsieh WT, Chung JG. Berberine induces cell cycle arrest and apoptosis in human gastric carcinoma Snu-5 cell line. World J Gastroenterol. 2006;12(1):21–8.
34. Athar M, Chaudhury NK, Hussain ME, Varshney R. Hoechst 33342 induces radiosensitization in malignant glioma cells via increase in mitochondrial reactive oxygen species. Free Radic Res. 2010;44(8):936–49.
35. Jaruga E, Salvioli S, Dobrucki J, Chrul S, Bandorowicz-Pikula J, Sikora E, *et al*. Apoptosis-like, reversible changes in plasma membrane asymmetry and permeability, and transient modifications in mitochondrial membrane potential induced by curcumin in rat thymocytes. FEBS Lett. 1998;433(3):287–93.